Experimental Investigation of The Steady Motion of Spherical- Cap Bubble

Mohsin Abbas Mashay * & Hussein Ali Hussab*

Received on: 2/11/2009
Accepted on:1/4/2010

Abstract

The aim of the present work is to study the hydrodynamics of spherical-cap bubble, rise bubble velocity, shape of bubble, and drag coefficient. The experimental work of two-phase ,air-water system was carried out using a Perspex column of 14.5 cm diameter and 180 cm height. A known volume of air was supplied to the cup from a syringe. The single gas bubble rose through the entrance region by turning the cup instantaneously. The rise bubble velocity was measured by visual observation. In order to measure the terminal velocity an electronic timer (Stop-Watch) was used. The drag coefficient of air spherical-cap bubble rising in water was measured and found to be a value between (2.8-3.8) for all Reynolds number. The experimental results are compared with the theoretical results of some investigators.

Keywords: Tow-phase; Bubbly flow; Large bubble; Drag coefficient

التحقيق التجريبي للانسياب المستقر للفقاعة الشبة كروية

الخلاصة

الغرض من البحث هو دراسة هايدروديناميكية الفقاعات الشبة كروية وذلك باستخدام تجارب عملية تضمنت قياس السرعة وشكل الفقاعة وقوة الجر. تم دراسة حركة الفقاعة الشبة كروية المفردة خلال السائل الساكن (الماء) وذلك باستعمال عمود من نوع البرسبيكس قطره الداخلي 14,5 سم وارتفاعه 180 سم مملوء بالماء.تم توليد الفقاعة الشبة كروية عن طريق حقن الهواء من أسفل العمود بواسطة محقنه وتجميعه في إل cup ثم يدور إل cup للحصول على الفقاعة.تم قياس سرعة الفقاعة بالاعتماد على المشاهدة البصرية وباستخدام ساعة توقيت .وجد إن قيمة معامل الجر للفقاعة الشبة كروية يساوي (2,8- 3,8) لكل قيم رينولد.
تم مقارنة النتائج التي تم الحصول عليها عمليا مع النتائج النظرية للباحثين الآخرين.

* Ministry of Science & Technology/ Baghdad

https://doi.org/10.30684/etj.28.12.4
2412-0758/University of Technology-Iraq, Baghdad, Iraq

Introduction

The motion and effects of bubbles are of great importance in many modern industrial applications examples of these application are: flow of immiscible fluids in vertical passages or tubes, fluidized beds, absorption of gasses in liquid columns, fermentation, agitation, stirring, sewage purification processes and direct contact heat exchangers[1].

Considering a bubble which rises in an infinite extended liquid three types of bubbles can be observed: spherical, spherioidal and spherical-cap bubbles . Which shape the bubble assumes depends on the ratio between the forces acting on the bubble surface[2]. A spherical-cap bubble which represents the last stage of evolution of bubble shape, finds important applications fields as diverse as metallurgy and de-icing of harbors, they appear in fluidized beds[3].

Davies and Taylor[4] photographed the air bubbles formed in nitrobenzene and showed that the greater part of the upper surface is always spherical. A theoretical discussion , based on the assumption that the pressure over the front of the bubble is the same as that in ideal hydrodynamic flow round a sphere, shows that the steady state velocity seems to be independent of liquid properties and is related to the radius of curvature R, in the region of the vortex , by the equation:

$$U_B = \frac{2}{3}\sqrt{gR} \quad \ldots\ldots\ldots\ldots\ldots\ldots\ldots(1)$$

Collins obtained a second approximation to the velocity of a large bubble using a perturbation analysis to balance the pressure along the interface as follows[5]

$$U_B = 0.652\sqrt{gR} \quad \ldots\ldots\ldots\ldots(2)$$

Which is in slightly in better accord with experimental values.

Haberman and Morton[6] obtained an almost identical result but expressed the velocity in terms of the equivalent radius (r_e) as :

$$U_B = 1.02(gr_e)^{1/2} \quad \ldots\ldots\ldots(3)$$

Collins[7] introduced a scale factor correction into the Davies-Taylor relation:

$$U_B = 0.71\sqrt{gd_e}\,SF \quad \ldots\ldots\ldots..(4)$$

Where

$$SF = 1 \quad \text{for } \frac{d_e}{D_T} < 0.125 \quad \ldots.(5)$$

$$SF = 1.13exp\left(\frac{-d_e}{D_T}\right)$$

$$\text{for } 0.125 < \frac{d_e}{D_T} < 0.6 \quad \ldots\ldots\ldots(6)$$

$$SF = 0.496\sqrt{\frac{D_T}{d_e}} \quad \text{For} \frac{d_e}{D_T} > 0.6..(7)$$

Krishna , Urseanu , Baten and Ellenberger[8] measured the rise velocity of single spherical cap bubbles and showed the conform exceeding well with the calculating using equation (4) and (6).

Yamamoto and Ishii[9] measured photo electronically by the digital counter the rise velocity of air spherical cap bubbles in the distilled water and 5 and 10 ppm of aqueous sodium laurly sulfate and poly oxyethlene monostearate solution. This paper was the first to report measurement of rise velocity using photo electronic technique.

Some investigators obtained experimental results for rise velocity of spherical cap bubble as a function of radius of curvature of the leading surface[10].

Wegener and Parlange[3] noted close agreement of the rise speed at a given volume for a remarkable variety of fluids ranging in density from water to mercury , and with viscosities of less than (1) to about (100cp).

The rise of the bubble in the stagnant liquid experiences a drag force, as in the case of the solid particles, which may be defined by the following equation :

$$F_D = \frac{1}{2} C_D \rho_L U_B^2 S_B \quad \dots\dots\dots\dots(8).$$

$For\ \theta_m = 50^\circ$ and (Re>150,Eo≧40)

the drag coefficient is represented by the equation[10]

$$C_D = \frac{4}{3}\frac{g d_e}{U_B^2}\frac{\Delta\rho}{\rho_L} = \frac{8}{3} \quad \dots\dots\dots(9)$$

The present work is to investigate experimentally the steady motion of spherical cap bubbles in an air- tap water , the rising bubble velocity and drag coefficient with different gas volume are presented.

Experimental

Fig.(1) shows a schematic diagram of the experimental apparatus. The bubble column was a cylinder of an inside diameter of (14.5)cm and a height of (180)cm.

The column was made of Perspex to enable visual observation of the bubble motion. Air was injected from a graduated syringe into a steel cup, shaped as a half-sphere of volume (145)cm^3,fitted in the water space, and stored under the cup. The single gas bubble rose through the entrance region by turning the cup instantaneously . The rise bubble velocity was measured by visual observation . In order to measure the terminal velocity visually an electronic timer (stop-watch) was used to determine the time of rise of the bubble between two fixed points (100)cm apart. The cylindrical column was filled with tap water of the properties given in table (1) . The water was kept at room temperature which varied very little through the day and was measured by an immersion thermometer.

The room temperature was ≈25°c . The operating pressure was atmospheric .

Experimental calculation of the drag coefficient

Consider a spherical cap bubble rose in stagnant liquid as shown in fig.(2) .

Force balance :

$$F_B = F_L + F_g \quad \dots\dots\dots\dots(10)$$

The buoyant force is

$$F_B = V_B \rho_L g \quad \dots\dots\dots\dots(11)$$

The drag force is

$$F_D = \frac{1}{2} C_D \rho_L U_B^2 S_B \quad \dots\dots\dots(12)$$

$$F_g = \rho_G V_B g \quad \dots\dots\dots\dots\dots(13)$$

We substitute equations (11,12,13) into equation (10) to get :

$$V_B \rho_L g = \frac{1}{2} C_D \rho_L U_B^2 S_B + \rho_G V_B g \,..(14)$$

Arrangement gives

$$C_D = \frac{4}{3}\frac{g d_e}{U_B^2}\frac{(\rho_L - \rho_G)}{\rho_L} \quad \dots..(15)$$

Results and discussion

The present experimental results for single spherical cap bubble rising in stagnant water are tabulated in tables (2),(3) . The time elapsed for the spherical cap bubble to rise between predetermined markers (100cm distance) was measured using stop-watch .

For each experiment one single air bubble was injected at the bottom of the column using a standard medical syringe (syringe of different capacities were used in order to cover a wide range of bubble diameter).Single bubbles ranged in volume from 3 to 145cm^3 .

For a bubble rising in an infinite medium, it is possible to prepare a generalized graphical map in terms of Eo, Mo, and Re numbers[11].The present experimental results , are projected in graphical map Figure (3) and it is shown that the present air bubbles are located in the spherical cap region .

The experimental spherical cap bubble shapes are shown in Figure (4) .

The photographs were recorded by a video recorder and appeared on the monitor , we note the greater part of the upper surface is spherical and this is in agreement with Davies and Taylor[4].

The present experimental values of the rise bubble velocity are compared with the theoretical values obtained from equations (1,2,3,4 and 6) .Figure (5) shows this comparison , the experimental rise velocity is in agreement with the theoretical predictions up to (R=4) but becomes less than the predictions at larger radii .

This case was also found by Krishna, Urseanv, Baten and Ellenberger[8].

The calculation of the curvature radius (R) of spherical cap bubble is based on the wake angle (Θ_m=50°) according to the empirical equation

$$\Theta_m - 50 + 190\exp\left(-0.62 R_e^{0.4}\right)$$

For $E_o \geq 40, R_e > 1$ .....(16)

and there is no theoretical prediction for the angle subtended by a spherical cup bubble but observation indicates that this is usually close to 50° [12].

Equation (1) does not give any information on the relationship between rise velocity (U_B) and volume of bubble (V_B) , unless the angle Θ_m of the cap is known . A value of Θ_m of about 50 degree would correspond to the following relationship among the curvature radius R and the bubble volume[13] :

$$R = 1.44\, V_B^{1/3} \;\ldots\ldots\ldots\ldots\ldots\ldots\ldots.(17)$$

Substituting equation (17) into equation (1) gives

$$U_B = 25.0\, V_B^{1/6} \;\ldots\ldots\ldots\ldots\ldots.(18)$$

The present experimental values of the rise bubble velocity are compared with the theoretical values obtained from equation (18) .

Figure (6) shows this comparison, the experimental velocity is slightly less than predicted by equation (18),this is in agreement with Gianni[13].

The drag coefficient in the higher Reynolds number region is independent of it. This seems to be certainly one of the aspects of the transition to the Taylor regime where the drag coefficient is constant .

Figure (7) shows the experimental results of the drag coefficient as a function of Reynolds number , the drag coefficient is constant in the case of large gas bubble.

Conclusions

The following conclusions are drawn from the present study:

- The spherical cup bubble shapes are photographed and found that the greater part of the upper surface is always spherical.
- The dimensionless groups for bubble , Re, Eo, and Mo are projected on the generalized map and show that the present air bubbles are located in the spherical cap region.

- The rising velocities of the spherical cap bubbles in water are .measured experimentally and found to agree with the following relation:

$$U_B = 0.71\sqrt{g d_e} SF \ldots (4)$$

and

$$SF = 1.13 \exp\left[\frac{-d_e}{D_T}\right] for\ 0.125 < \frac{d_e}{D_T} < 0.6 \ldots (6)$$

- The drag coefficient of spherical cap bubble rising in water is measured and found that to be a value between (2.8-3.8) for all Reynolds number .This is in agreement with most investigators.

Nomenclature

C_D Drag coefficient, dimensionless
d_e Equivalent diameter of spherical cap bubble (m)
D_T Cylindrical column diameter (m)
E_O Eotvos number $\left(g d_e^2 \frac{\rho_L}{\sigma}\right)$
F_B Buoyancy force (N)
F_D Drag force (N)
g Acceleration due to gravity (m/s^2)
M_O Morton number $(g \mu_L^4 / \rho_L \sigma^3)$
R Frontal radius of curvature of spherical cap bubble(m)
r_e Equivalent radius of spherical cap bubble (m)
Re Reynolds number $\rho_L d_e U_B / \mu_L$
S_B projected area of a gas bubble (m^2)
SF Scale correction factor, dimensionless
U_B Rise velocity of a bubble (m/s)
V_B Spherical cap bubble volume (m^3)
θ_m Maximum angle of spherical cup bubble (deg.)
σ Surface tension (N/m)
ρ_G Density of gas phase (Kg/m^3)
ρ_L Density of liquid phase (Kg/m^3)

References

[1]. Kendoush, A. A., "Theory of Convective Heat and Mass Transfer to Spherical-Cap Bubbles", AIchE J., 40, 9 [1994].

[2]. Coppus, J. H. C, and Rietema, K., "Description of Bubble Shape in Term of Dimensionless Numbers", 35, 1497 [1980].

[3]. Wegener, P. P., Parlange, J. Y., "Spherical-Cap Bubbles", Ann. Rev. Fluid Mech., 5, 79 [1973].

[4]. Davies, R., and Taylor, G. I., "The Mechanics of Large Bubbles Rising through Extended Liquids and through Liquid in Tubes", Proc. Roy. Soc. (London), A200, 375 [1950].

[5].Collins, R., "A second Approximation for the velocity of a Large Gas Bubble Rising in an Infinite Liquid", J. Fluid Mech., 25, 469 [1966].

[6]. Haberman, W. L., and Morton, R. K., "An Experimental study of Bubbles Moving in Liquids", Amer. Soc. Civil Eng. Trans., 121, 227 [1956].

[7].Collins, R., "The Effect of a Containing Cylindrical Boundary on the Velocity of a Large Gas Bubble in a Liquid", J. Fluid Mech., 28, 97 [1967].

[8]. Krishna, R., Urseanu, M. I., Van Baten, J. M., and Ellenberger, J., "Rise Velocity of a Swarm of Large Gas Bubbles in Liquids", Chem. Eng. Sci., 54,171 [1999].

[9]. Yamamoto, Y., and Ishii, T., "Effect of Surface Active Materials on the Drag Coefficients and Shapes of single Large Gas Bubbles", Chemi. Eng. Sci, 42, 6 [1987].

[10].Clift, R., and Grace, J.R., and Weber, M.E., "Bubbles, Drops and Particales", Academic press, New York [1978].

[11]. Grace, J. R.,"Trans. Inst. chem. Eng., 51, 116-120 [1973].

[12]. Stanley, M., "An introduction to fluid dynamics", New york [1998].

[13]. Gianni, A., and Gennaro, A., "Motion of Gas bubbles in Non-Newtonian Liquids", A. I. ch. E Journal, 11,815 [1965].

Table (1) Water properties at~25 ^{o}c.

Liquids	ρ kg/m^3	μ x 10^3 $N.s/m^2$	σ N/m	Morton Number
Water	997.0	0.890	0.072	1.73 x 10^{-11}

Table (2) Times of spherical –cap bubbles through rise in column

Volume Cm^3	Time S	Volume Cm^3	Time S
3	3.47	15	2.72
4	3.31	16	2.70
5	3.21	17	2.66
6	3.09	18	2.64
7	3.03	19	2.63
8	2.96	25	2.56
9	2.92	30	2.51
10	2.87	40	2.41
11	2.81	50	2.36
12	2.78	75	2.27
13	2.76	100	2.19
14	2.75	145	2.09

Table (3) Experimental results of spherical-cap bubbles at different volumes.

Air-Water

$M_o = 1.73*10^{-11}$

Exp No.	Volume of gas Cm^3	$d_e = \left(\frac{6V_B}{p}\right)^{1/3}$	R_e	E_o	C_D
1	3	1.789	5775.76	43.48	2.8139
2	4	1.969	6663.49	52.67	2.8186
3	5	2.122	7404.719	61.17	2.8570
4	6	2.255	8174.48	69.08	2.8133
5	7	2.373	8772.37	76.49	2.8468
6	8	2.481	9388.39	83.62	2.8405
7	9	2.581	9902.70	90.49	2.8744
8	10	2.673	10432.35	97.06	2.8769
9	11	2.759	10999.80	103.40	2.8456
10	12	2.841	11447.66	109.64	2.8686
11	13	2.917	11838.86	115.59	2.8825
12	14	2.990	12178.68	121.44	2.9546
13	15	3.060	12600.91	127.19	2.9584
14	16	3.126	12970.75	132.74	2.9767
15	17	3.190	13432.85	138.233	2.9494
16	18	3.252	13799.57	143.66	2.9608
17	19	3.311	14101.86	148.92	2.9924
18	25	3.628	15874.67	178.79	3.1066
19	30	3.855	17204.77	201.87	3.1729
20	40	4.243	19720.67	244.56	3.2200
21	50	4.571	21695.76	283.83	3.3264
22	75	5.232	25817.77	371.85	3.5226
23	100	5.759	29456.97	450.53	3.6087
24	145	6.518	34938.27	577.11	3.7190

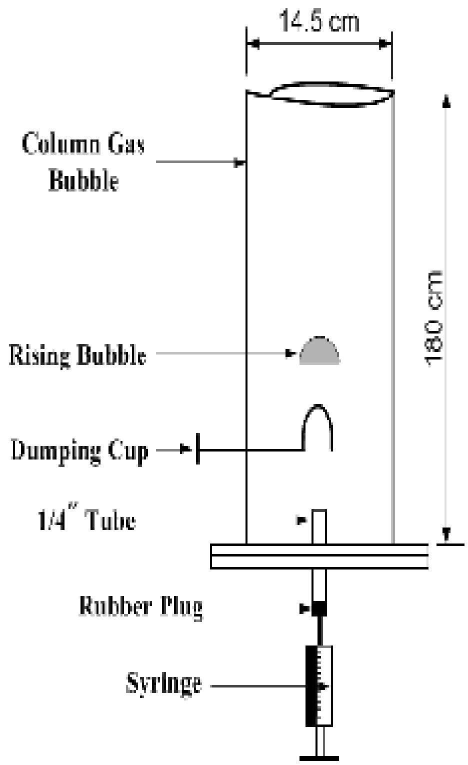

Figure (1) Schematic Diagram of Experimental Spherical-Cap Bubble

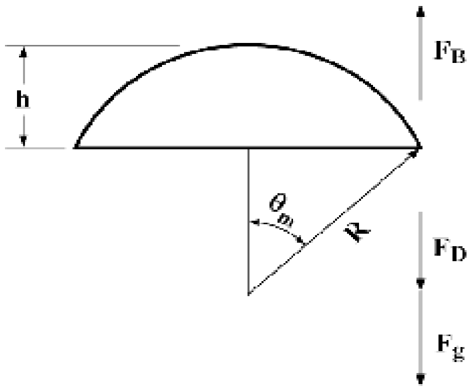

Figure (2) Geometry of Spherical-Cap Bubble

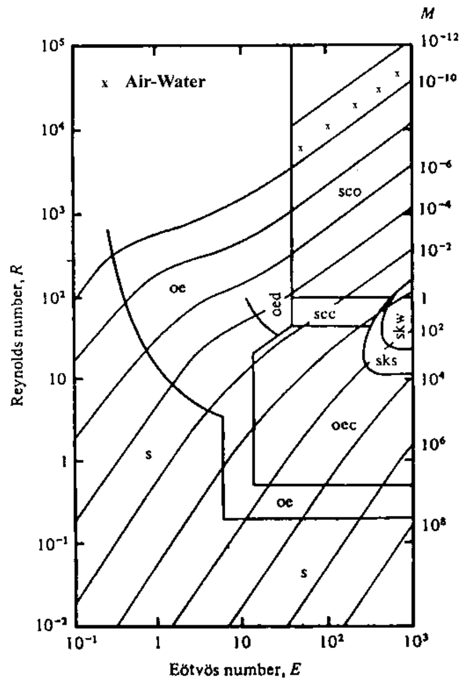

Figure (3) The present experimental results are compared with the shape regimes for bubble in rising through liquids

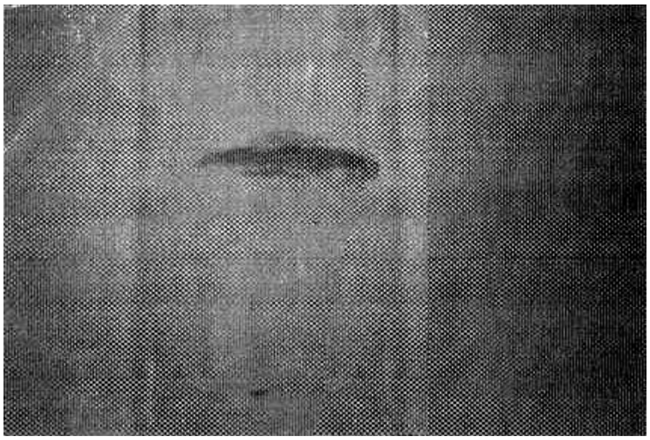

Figure (4) Spherical-Cap bubble

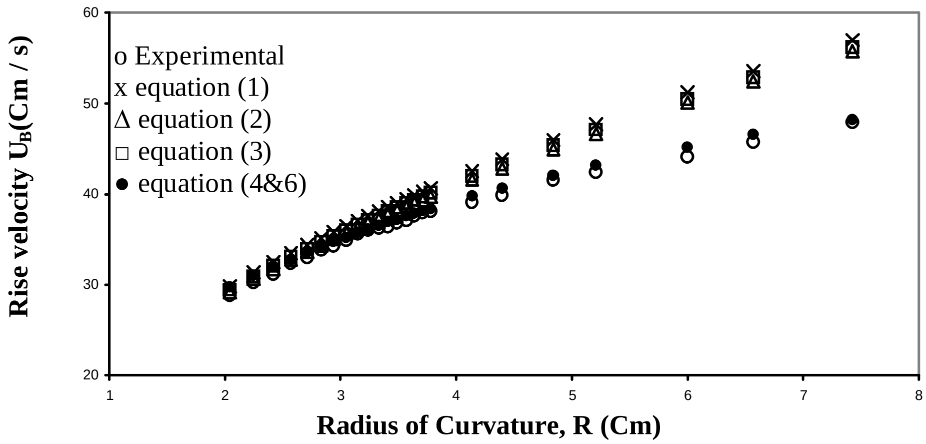

Figure (5) Rise velocity of spherical cap bubble as a function of the radius of curvature.

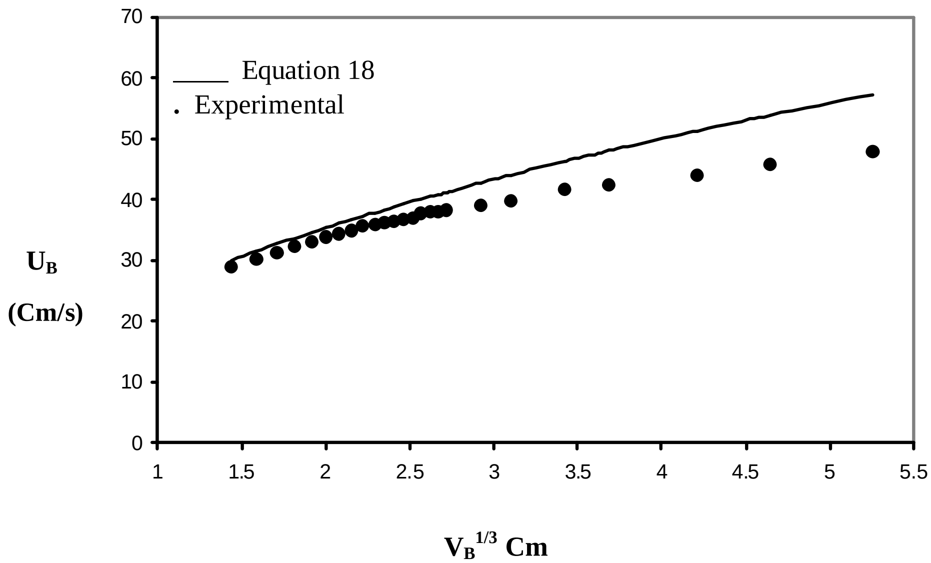

Figure (6) Experimental Rise speed of spherical-cap bubble as a function of the bubble volume

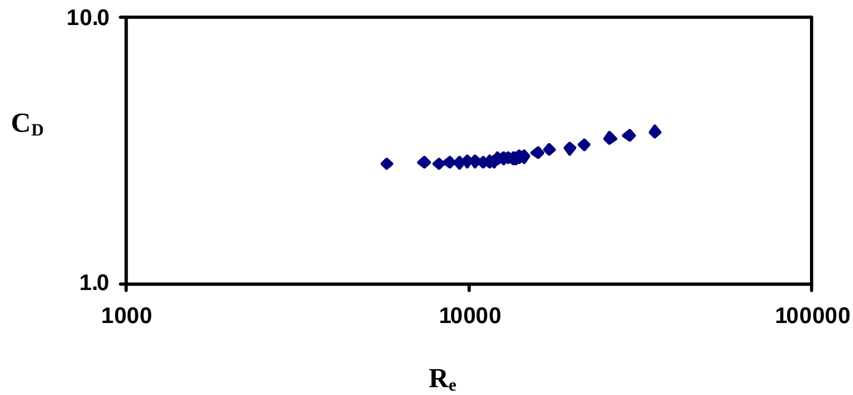

Figure (7) Drag coefficient of spherical-cap bubble as a function of Reynolds Number